ON-GROUND VERIFICATION OF VIBANASS (VISION BASED NAVIGATION SENSOR SYSTEM): CAPABILITIES AND RESULTS

Q. Mühlbauer, P. Rank, C. Kaiser
Kayser-Threde GmbH, Wolfratshauser Strasse 48, 81379 Munich, Germany
Email: {quirin.muehlbauer, peter.rank, clemens.kaiser}@kayser-threde.com

ABSTRACT

A versatile optical Rendezvous, Docking and Landing (RVDL)-camera system including an illumination subsystem is developed and verified in the VIBANASS project. A demonstrator model representative with regard to the flight hardware was built for execution of a space qualification programme. Although technical requirements for VIBANASS have mainly been derived from LEO and GEO missions, lunar missions can also be served.
During an extensive test campaign at EPOS it was shown that VIBANASS is able to serve as sensor for safe vision-based Rendezvous and Docking Maneuvers under a wide variety of environmental conditions.

1. INTRODUCTION

This paper gives an insight into the VIBANASS [2,5] project with a strong emphasis on latest results of an intensive test campaign at the new European Proximity Operations Simulator (EPOS) [3] at DLR (Deutsches Zentrum für Luft- und Raumfahrt). In detail, VIBANASS comprises two Camera Systems (CS), a Target Illumination System (TIS) and a Ground Operation System (GOS). Each Camera System includes three cameras, optimized for far-range (3km to 75m), mid-range (500m to 4.5m) and close-range (5.5m to 0.7m). In close-range, two cameras are operated in a stereo configuration with a stereo base of 0.5m. The laser-based Target Illumination System is a highly modular assembly, supporting a wide range of different optical power configurations called for by the different application requirements. Possible applications of VIBANASS include the Orbital Live Extension Vehicle (OLEV) [1], which comprises a Servicer satellite with a robotic tool for capturing of a Client satellite, or DEOS (Deutsche Orbitale Servicing Mission) [7], a robotic servicing mission in LEO.
A first test campaign with a breadboard model of VIBANASS under representative illumination conditions has been conducted in December 2011 [4] at the EPOS facility. The feasibility of vision based navigation in close distance using VIBANASS could be shown with the results of this test campaign. A further test campaign was conducted in early 2013, using the final demonstrator model of VIBANASS. The campaign included functional and performance tests. Distance determination data of a dedicated image processing [6] ground software is used for verification and evaluation of the performance of VIBANASS. The software applies target specific distance estimation algorithms and uses the VIBANASS camera images as input. It was not only used for evaluation of the performance, but also served as input for a closed-loop RVDL control algorithm in an additional test.

2. VISION BASED NAVIGATION SENSOR SYSTEM

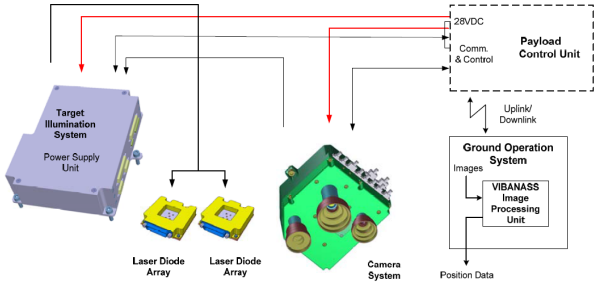

Figure 1. Operational Scenario of VIBANASS

Fig. 1 shows the operational scenario of VIBANASS with one Camera System (CS), the Target Illumination System (TIS) and the Ground Operation System (GOS) in flight configuration. VIBANASS equipment was designed for an operational temperature range of -40°C to +50°C and a non-operational range of -40°C to +85°C. Further, the design is radiation tolerant (TID: 100 KRad(Si), LET: 80 MeV cm²/mg).
The subsystems of VIBANASS will be presented in detail in the next sections.

2.1. Camera System

The VIBANASS Camera System comprises all necessary hardware for the operation of three CMOS Sensors, communication interfaces, hardware controller and a power-supply module. Further, each camera system supports a resolution of up to 1024x1024 pixels, real-time JPEG compression and is optimized for a communication bandwidth between 400kbit/s and 4Mbit/s. A common housing accommodates all electronics and optics for the three different camera heads. Core functions and features of the Camera System are:

- redundant SpaceWire Inteface Encoder/Decoder

- individual control of each camera head
- Synchronisation for stereo camera
- Image acquisition rate: max. 10Hz
- Lossy and lossless JPEG compression
- Configurable image size
- Synchronisation with Target Illumination System
- Simultaneous operation of 2 camera heads (stereo image acquisition)
- Optional Image Processing Module (internal Add-on Module for image pre-processing functions)
- Power consumption: 28 V / 5 W
- 4.8 kg for GEO application and 3.7 kg for LEO
- Size of CS: 250.5mm x 236.5mm x 215.1mm

2.2. Target Illumination System

The laser-based VIBANASS Target Illumination System (TIS) is designed to illuminate the whole filed of view of the VIBANASS Close-Range Camera over a distance of 5m with an optical power of at least 10% of natural sunlight. Therefore the Close-Range Camera's spectral bandwidth corresponds to the wavelength (808nm) of the laser-based illumination system within the specified environment. Due to its modularity, other applications can also easily be served.
A TIS Module consists of a Power Supply Unit (TIS-PSU) and two Laser Diode Arrays (TIS-LDA) with 8W optical power for each. Several TIS modules can be operated in parallel. Using dedicated hardware lines the TIS power output can be synchronized with the VIBANASS Camera System for energy saving. Furthermore, the output power can be remotely controlled by digital control. Isolated safety inhibit signal lines support ground operation safety.
The TIS-LDA was successfully tested with a TID of 235 KRad(Si) and with 3.1E11 protons/cm2 @ 30MeV. Its physical parameters are:
- Size of TIS-PSU: 169 mm x 106 mm x 40 mm
- Size of TIS-LDA: 70mm x 76mm x 20mm
- 2.05 kg (incl. 2 LDAs) for GEO, 1.65 kg for LEO
- Power consumption: 28 V / 15 W @ 16W optical power and 10% duty cycle

2.3. Ground Operation System

In addition to the hardware, the Ground Operation System (GOS) comprises software to command the VIBANASS equipment, to receive and decompress images and finally to estimate the position of the target in real-time. For this purpose, it performs frame-to-frame tracking by using a geometric model, and it is capable of automatic re-initialization in case of loss.
Object detection consists of a global search, in order to localize the given shape (rectangle, circle) in full 3D space, within the whole range of distances and horizontal, vertical positions [6]. This procedure is computationally intensive and less accurate than tracking, and can also provide false positives (the object is found in the wrong location) or missing detections.
The tracking procedure, instead, consists of a local search, that requires a predicted pose. In absence of a dynamical model, the prediction is simply given by the estimate from the previous frame. The edge-based tracking procedure is based on a local search for nearest-neighbor edges, along the normals to the contour. Least-squares errors are minimized using a robust estimator and the procedure is iterated until convergence.

3. TEST SETUP

The general test setup is shown in Fig. 2, comprising the target mockup (left robot) and the VIBANASS equipment mounted on the right robot. This robot is mounted on a rail for the movement in line-of-sight direction. The sun simulator is shown on the right side of the image, a 12kW spotlight with a sun like spectrum and comparable optical power.

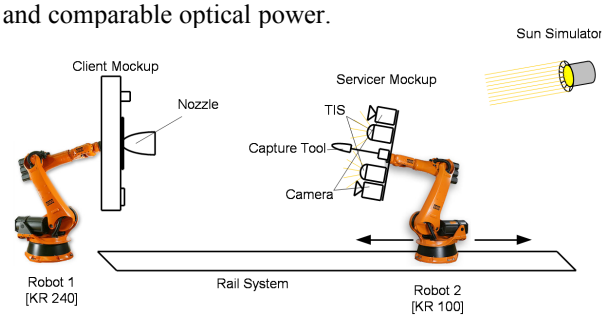

Figure 2. General Test Setup

Fig. 3 shows the setup with the two VIBANASS cameras and parts of the Ground Operation System:
- Two Camera Systems, mounted on the top left and on the top right
- Capture Tool, a servicing tool on the chaser satellite
- TIS-Power Supply Unit, mounted on the bottom right
- Two TIS-LDAs, mounted between the Camera Systems and between the TIS-PSU and the GOS
- Ground Operation System, mounted on the bottom left

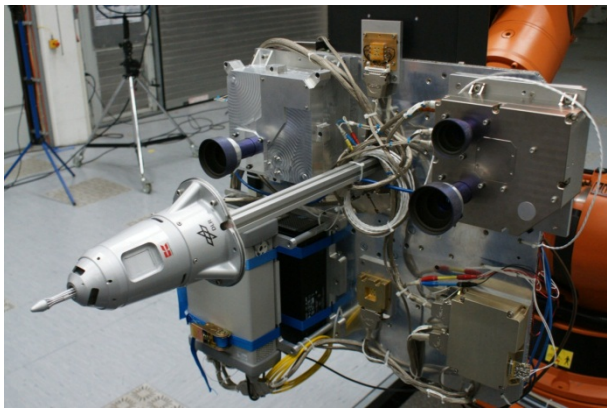

Figure 3. VIBANASS mounted on the chaser

Both Close-Range Cameras are used as a stereo camera system with a stereo base of 0.5m. The Ground Operation System mounted on the robot is composed by a computer and the digital interface, emulating an on-board computer on a satellite. Results of the image processing algorithm are computed in a reference frame located in the focal point of the left Close-Range Camera for the stereo case and in the focal point of the left Mid-Range camera for the mono case. The line of sight marks the z-axis and the camera horizon marks the x-axis.

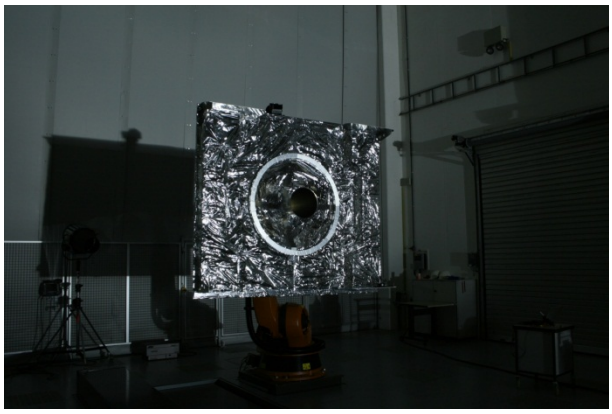

Figure 4. Target Mockup

Fig. 4 shows the mockup of the target, which is illuminated by the sun simulator. The target frame is located in the center of the nozzle's exit-plane.
Different trajectories as described in Tab. 1 have been used for the tests, starting at a distance of 25m and ending at the parking position at a distance of 0.5m. The distance is measured in z-direction between the camera frame and the target frame.

Table 1. Description of the trajectories

ID	Description	Duration
N1	Linear movement from 25m to 0.5m Station keeping for 120s at a distance of 5m	~15 min
N2	N1 + sinusoidal rotation around the y-axis	~13,5 min
N3	N2 + linear rotation around the z-axis	~13,5 min
S1	Fixed position at 5m, Sinusoidal rotation around the y-axis	~5 min
S2	S1 + sinusoidal movement in y-direction	~5 min

Those trajectories cover nominal as well as non-nominal cases and are used under different illumination conditions. The linear movement in N1 covers the nominal case, while the movements with a relatively large displacement in N2 and the sinusoidal oscillation around the y-axis in N3 mark the non-nominal cases, imposing a challenge to the robustness of the image processing. Further, all trajectories are accelerated by a factor of 5 against real mission conditions which increases the number of illumination conditions that can be tested in a reasonable amount of time. The image processing algorithm is expected to have a larger error in the non-nominal cases, while the image quality remains constant. The different trajectories were simulated with four different positions of the sun simulator and with five different illumination settings.

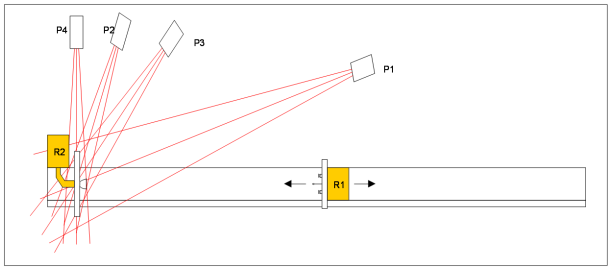

Figure 5. Different positions of the sun simulator

Fig. 5 shows the four different positions of the sun simulator. The positions differ in the angle between the camera line of sight and the sun simulator. In addition to, a test case without the sun was defined.

Table 2. Achieved ratio between sun simulator and Target Illumination System

Desired Ratio	20%	10%	5%
Sun irradiance [W/m²]	8.1	11.9	15.9
TIS irradiance [W/m²]	1.64	1.13	0.73
Achieved ratio	20.2%	9.5%	4.6

Before performing the actual tests the illumination conditions have been calibrated. Therefore the sensor head of an optical power meter was mounted on the target mockup, the sun simulator was placed at the given positions and the brightness was adjusted, until the desired ratio between the irradiance achieved by the sun simulator and the irradiance achieved by the Target Illumination System was measured. In a real setting, the Target Illumination System is able to illuminate with an optical power of 10% of the sunlight at a distance of 5m. This value was estimated by a radiometric analysis and verified during the first breadboard test campaign at EPOS. Tab. 2 shows a list of the optical power of the Target Illumination System and the sun simulator.

Table 3. Selection of the 53 test cases

Nr.	Trajectory	Sun	Illumination
T 1.1	N1	P1	20%
T 1.9	N1	P1	5%
T 1.14	N1	P1	No Sun Sim.
T 1.20	N1	P1	No TIS
T 1.36	N1	P3	20%
T 1.53	N1	P4	No TIS

A total of 53 test cases shown in Tab. 3 have been selected for the tests, varying the trajectory, the position of the sun and the illumination setting. Thus, a wide variety of environmental conditions is achieved.

Fig. 6 shows the approach of trajectory N1 at a distance of 15m and 0.5m as seen by a surveillance camera. The surveillance camera is sensitive to infrared light, so the operator is able to see the laser of the TIS.

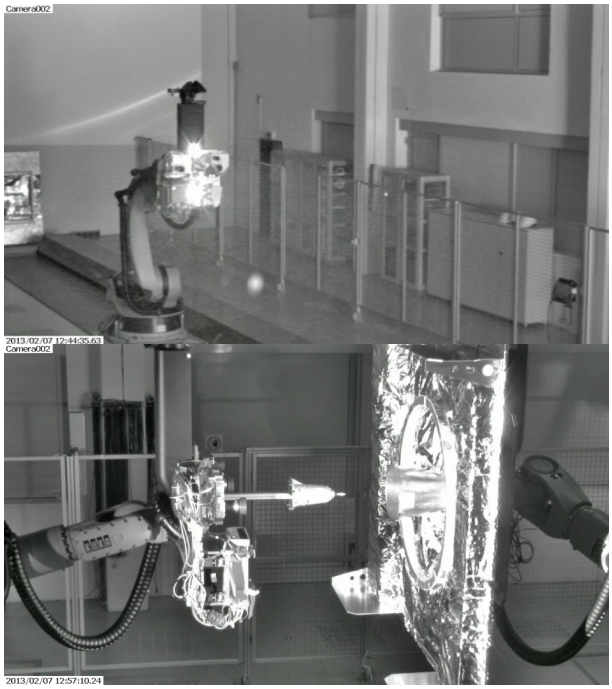

Figure 6. Approach seen by a surveillance camera

4. TEST RESULTS

This section describes the major results from the EPOS tests, starting with example images recorded by the Camera System under different illumination conditions and configurations. Image quality and performance of the image processing algorithm are evaluated, followed by a brief summary of the closed-loop tests.

4.1. Example Images

Fig. 7 compares images recorded by the Close- and Mid-Range Camera under good and bad illumination conditions. The images have been recorded at distances of 5m and 2m by the Close-Range Camera and the Mid-Range Camera, respectively.

Fig. 8 shows the impact of the image compression for the Close- and the Mid-Range Camera. The left column shows images with a high compression and the right with a low compression setting. As expected, high compression leads to a poor image quality. The difference between lossless and low compression rates cannot be recognized by the human eye. All images have been recorded at a distance of 5m for the Close-Range Camera and 20m for the Mid-Range Camera.

Low compression is optimized for sending a stereo image pair at full resolution with a communication bandwidth of 4Mbit, which is a typical for a LEO application. High image compression is optimized for a communication channel with a bandwidth of 0.4Mbit, a typical value for a chaser's S-Band link in GEO.

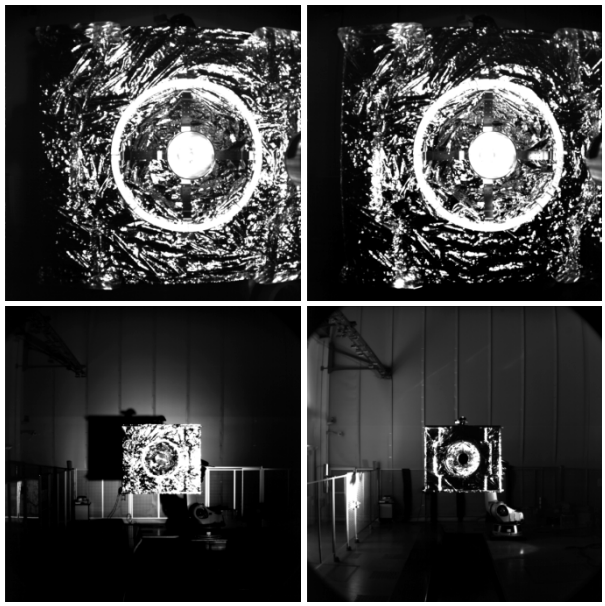

Figure 7. Good (left) and bad (right) illumination conditions seen by the CAM-CR (top row) and the CAM-MR (bottom row)

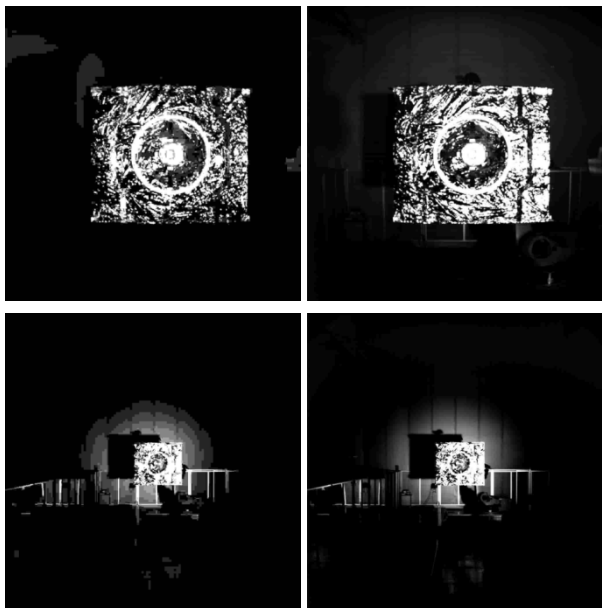

Figure 8. High (left) and low (right) image compression

Fig. 9 illustrates the impact of the TIS by showing images recorded under different brightness settings (from top left to bottom right): no active TIS, illumination ratio of 5%, illumination ratio of 20% and no sun simulator. Note that the exposure time has been adjusted to increase the overall image quality, so the brightness seems comparable. All images have been recorded at a distance of 5m.

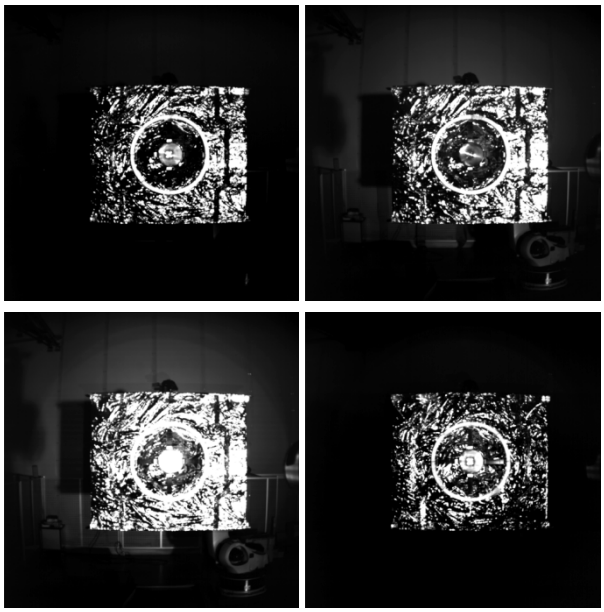

Figure 9. Impact of the TIS

Not only the quality of the images and the positions error of the image processing algorithm is important, but also the delay induced by the whole system. The results show, that the delay is depending on the compression rate and ranges between 350ms for an lossless image and 20ms for high compression.

4.2. Evaluation of Image Quality

A total of 53 test cases has been recorded during the EPOS tests. The following image quality factors have been analyzed for each image recorded during the tests:

- Signal to Noise Ratio
- Sharpness/blur
- Image contrast

For the evaluation of the image quality, the images have been separated into the target (structured parts of the image) and the background (smooth parts of the image, mostly black).

The image quality has been evaluated for each test case, which mainly differ in the illumination conditions. To permit a reliable statement, the test cases have been separated into three categories:

- All test cases are included in the category mean illumination conditions.
- Challenging conditions are combined in the category bad illumination conditions. Those include test sequences with no sun simulation, large angles between the line of sight and the sun simulator or failures in the TIS.
- Favorable conditions are those with the sun coming from the back and with nominal TIS. They are combined in the category good illumination conditions.

The signal to noise ratio of the cameras is measured in dB and is computed using the mean absolute deviation algorithm. Therefore the image is separated into small windows, in which the noise is assumed to be constant. The noise is reduced using a median filter and is then subtracted from the original image. The noise remains constant, while the signal is strongly depending on the visual context of the image, namely the distance to the target and the illumination conditions. Furthermore, the SNR was computed using an ISO 12233 pattern. A SNR of 56.7dB was computed for the Close-Range Camera and 58.4dB for the Mid-Range Camera. Naturally, this marks the maximal value and the SNR of the images recorded during the EPOS tests is well below.

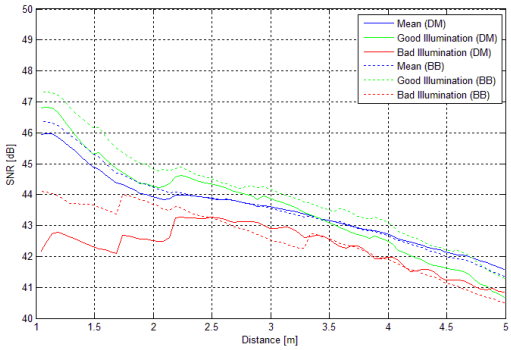

Figure 10. SNR over the distance for CAM-CR

Fig. 10 shows the signal to noise ratio of over the distance for the VIBANASS Close-Range Camera. The SNR increases with decreasing distance, as the camera is designed for distances shorter than 5m and the size of the target seen by the camera and thus the signal level increases. The blue line shows the mean SNR measured using all test cases, while the red line shows the SNR of the test cases with bad illumination conditions and the green line shows the SNR for favorable illumination conditions.

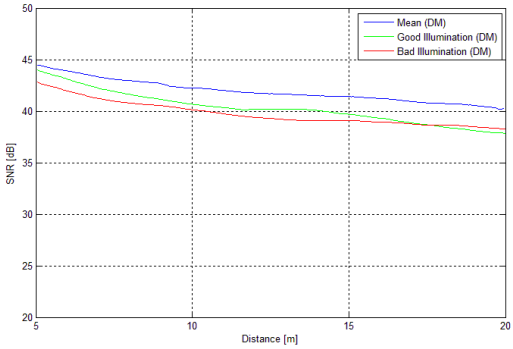

Figure 11. SNR over the distance for CAM-MR

Bad illumination conditions include situations with no Target Illumination System or with bad sun angles and therefore poor illumination of the target and thus a poor signal. In distances < 2.1m the chaser starts to shadow

parts of the target. This leads to a sudden decrease of the illumination conditions and a strong divergence between good and bad illumination conditions.
Fig. 11 shows the SNR for the Mid-Range Camera, which is designed for distances larger than 5m. Here, only a weak relation between the SNR and the distance can be identified. In contrast to the Close-Range Camera, the dependence on the illumination conditions is weaker, as it is easier to optimize the images by adjusting the exposure time. Further, the illumination conditions are more constant due to is less stray-light and shadows and on the target.
The sharpness of the Cameras and the image contrast are within the expected ranges. Sharpness is only depending on the distance, with the image contrast is mainly depending on the illumination environment.

4.3. Evaluation of Image Processing

This section describes the results of the image processing algorithm applied on the recorded test images. Before the actual image processing was performed, the cameras have been calibrated using a chessboard pattern. Based on the results of the calibration, the extrinsic and intrinsic camera parameters have been computed and applied during the image processing.

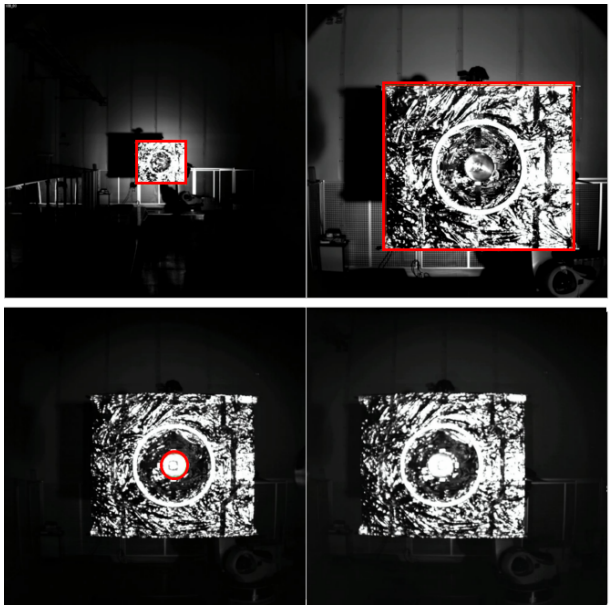

Figure 12. General results of image processing

Some general results of the tracking algorithm are shown in Fig. 12. The top row shows the results of the tracking in mid-range at 20m and at 5m, where the tracking target is the rectangular target shape. In close-range, the circular nozzle ring is the target of the tracking algorithm. As stereo images are used, the left and right camera images are shown at a distance of 5m. The additional delay induced by the image processing software was measured with 130ms in average.
For the actual evaluation of the image processing software, the stereo and the mono setup have been tested and the error between the estimations and the values recorded by EPOS has been computed. The relative error is defined as the relation between the position error in all three spatial dimensions with respect to the distance in percent.

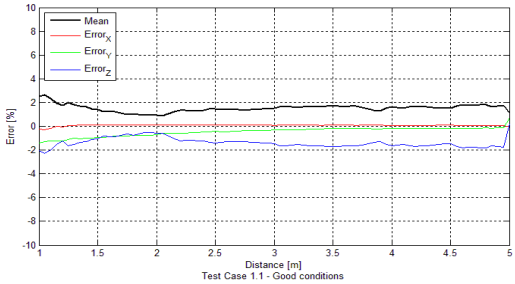

Figure 13. Result of tracking for good illumination conditions

Fig. 13 shows the resulting error of an approach under good illumination conditions. The relative error remains constant over the whole distance. In this case, the error ranges between 1% and 2%.

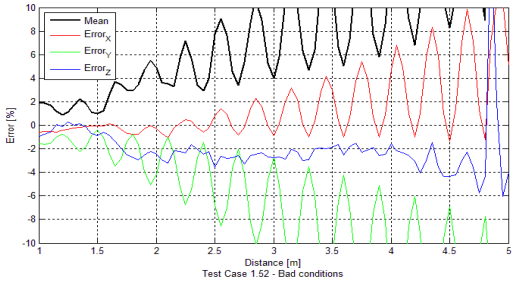

Figure 14. Result of tracking for bad illumination conditions

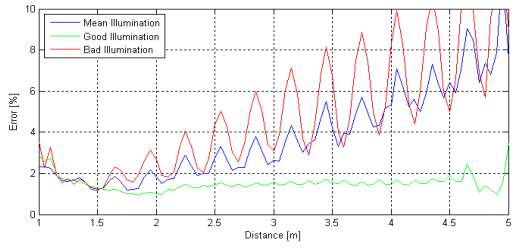

Figure 15. Impact on illumination conditions

An approach under bad illumination conditions is shown in Fig. 14. The absolute error is quite large and is further oscillating. Again, it decreases with decreasing distance. While the distance error in z-direction was dominant in test case T1.1 (see Fig. 12), the error in y-direction is dominant in this test case.

Fig. 15 shows the relative error for the stereo algorithm under good, bad and average illumination conditions. In all cases, the absolute error decreases with decreasing distance. The relative error has a more interesting behavior. It remains constant under good illumination conditions and decreases for average and bad illumination conditions.
The decrease can be easily be explained, as the irradiance of the Target Illumination System increases with decreasing distance and the TIS becomes more dominant compared to the sunlight. However, at distances < 2.1m the error begins to increase for all three cases. This behavior was also observed at the image quality factors and is explained by increasing straylight and shadows on the target induced by the chaser.

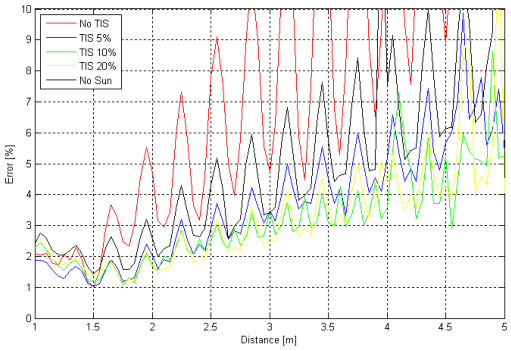

Figure 16. Impact of the Target Illumination System

The impact of the brightness of the TIS is shown in Fig. 16. "No TIS" shows the worst performance, while the active modes are comparable. When the target is illuminated only by the TIS, the resulting performance is slightly worse that when both, sun and TIS are active. These tests show that the TIS is mandatory for the image processing algorithm, as it significantly increases the brightness of the image, revealing more details of the target and illuminates shadowed parts.

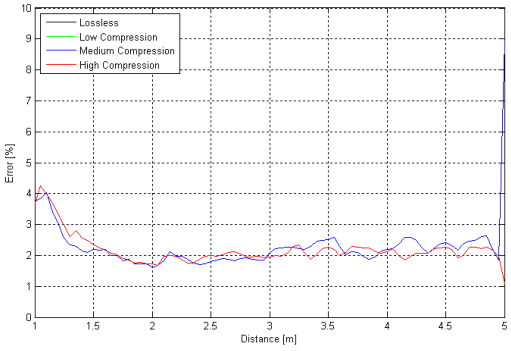

Figure 17. Impact of image compression

As described before, image compression has a large impact on the image quality. High compression rates as they are required for GEO applications such as OLEV, lead to large artifacts and a poor quality. Thus, the error of image processing under different image compression settings is of great interest.
Therefore several trajectories under good illumination conditions have been repeated with different compression settings. Fig. 17 shows the result of the stereo image processing algorithm in Close-Range. The resulting error is independent from the compression rate, proving that a vision-based approach is possible even with a small communication bandwidth.

4.4. Closed-Loop Tests

So far, trajectories have been run and the images have been recorded for later evaluation. The computed relative error was within the specified limits, so it was possible to use the result of the position estimation as input for additional closed-loop tests. Similar to the open-loop tests, EPOS was used to simulate the environment with realistic illumination conditions. A software based simulator has been integrated, containing dynamic models of the two satellites and a GNC system using the results from VIBANASS as input for its navigation filter. The dynamic model simulates an orbit controller, orbit actuators and sensors, orbit dynamics and kinematics, and delivers the position and pose of the two satellites, which was than used as input for the robot control of the EPOS facility, closing the control loop.
A modified version of the N1 trajectory was used for the closed-loop tests with decreased speed and a longer hold point at 5m. Due to safety reasons, the end point was moved to a distance of 2m between chaser and target. The switch between mid- and close-range was done manually.
A selection of seven different illumination conditions from the good and average conditions have been tested. In an additional test, the image processing software was replaced with an operator performing its tasks. In the OLEV scenario, manual operator guidance is used as backup in case of a failure of the image processing algorithm, e.g. caused by sudden inflexions between chaser and target surfaces.
During the image processing based closed-loop tests, the measurement error decreased with decreasing distance and the position error induced by the time delay increases with increasing velocity. During the whole processing loop, a time delay of ~1second was measured. As the dominating movement is in z-direction, the time delay has a major effect on the error in z-direction and almost no impact to the error in x- and y-direction. The relative error in x- and y-direction was ~0.5%, while the measured total relative error was <2% at all distances.
The test has been repeated with an operator in the loop,

leading to more challenging conditions for the control algorithm. As the target is hard to track for the human eye, the operator delivers less accurate results, especially at large distances. Further, changes of the target size are small between two consecutive images and the operator not always updates his measurement with every image, leading to a reduced measurement rate of about 0.2 – 0.3Hz in average, while positive and negative measurement errors alternated. In mid-range, the rate was even reduced to <0.1Hz in some cases. The experiment has shown that it is hard for the operator to concentrate during the whole approach, so it might be reasonable to use two operators in a real scenario.
Despite the harsh condition during the operator in the loop, a stable approach could be accomplished. Thus, it could be proven that vision-based sensors as VIBANASS can be used as navigation sensors for Rendezvous and Docking applications, even with a low communication bandwidth such as 400kbit.

5. SUMMARY

The VBIANASS Demonstrator Model tests at the European Proximity Operations Simulator (EPOS) have been completed with great success, as the Camera System DM, the Target Illumination System DM and the Ground Operation System have been tested successfully.
The analysis of the image quality has shown that the quality is strongly depending on the illumination conditions and the distance between target and chaser. The image quality meets the requirements under average and favorable illumination conditions. During the tests, it could be shown that the Target Illumination System is required to achieve sufficient image quality. Further optical tests have been conducted to successfully verify further requirements, like the field of view of the Close-Range and the Mid-Range Camera.
An analysis of the impact of the illumination conditions on the accuracy of the tracking algorithm has shown, that the Target Illumination System improves the natural illumination conditions such that the distance determination requirements can be fulfilled. Under good illumination conditions, the tracking algorithm is able to estimate the position of the target with an accuracy of ~1%. The image quality is strongly depending on the image compression. However, the tracking algorithm is still able to estimate the positions with an adequate error using highly compressed images, as they occur during GEO missions. The principle applicability of VIBANASS for Rendezvous and Docking Maneuvers could be verified with the image processing algorithms during the test campaign. For further real applications, the tests should be enhanced and repeated based on the presented results and a subset of test cases with realistic speed.
Finally, the functionality of VIBANASS and the image processing software could be proven during additional closed-loop tests. During these tests, the result of the image processing algorithm has been used as control input for a rendezvous simulator, showing stable results. It could be shown during the EPOS test campaign, that VIBANASS is capable to serve as an optical sensor for Rendezvous and Docking applications in mid- and close-range. The Target Illumination System significantly decreases the dependence on natural illumination, allowing to use VIBANASS under a wide variety of environmental conditions. Without the artificial illumination of the TIS, safe vision-based Rendezvous and Docking Maneuvers are not possible.

6. ACKNOWLEDGMENTS

VIBANASS is a Kayser-Threde development programme under co-funding by DLR (Förder-kennzeichen 50RA1001), the German Space Agency and in cooperation with DLR-RM (DLR Institute for Mechatronics and Robotics) and DLR-RB (EPOS). vH&S (von Hörner und Sulger) is subcontractor.

7. REFERENCES

1. Kaiser, C. & Sjöberg, F. & Del Cura, J. & Eilertsen, B. (2008). *SMART-OLEV—An orbital life extension vehicle for servicing commercial spacecrafts in GEO*, Acta Astronautica 63 (2008) 400 – 410

2. Rank, P. & Kaiser, C. (2010). *VIsion BAsed Navigation Sensor System VIBANASS*, AGASSE

3. Wimmer T., & Boge, T. & Mühlbauer, Q. (2011). *EPOS: A Hardware-in-the-Loop Robotic Simulation Assembly for Testing Automated Rendezvous and Docking GNC Sensor Payloads.* International ESA Conference on Guidance, Navigation & Control Systems

4. Mühlbauer, Q. & Richter, L. & Kaiser, C. & Hofmann, P. (2012). *Robotics Space Systems and Subsystems for Advanced Future Programmes* International Symposium on Artificial Intelligence, Robotics and Automation in Space (i-SAIRAS)

5. Kaiser, C. & Rank, P. & Landzettel, K. & Boge, T. & Turk, M. (2011). *Vision Based Navigation for Future on-Orbit Servicing Missions*, 62nd International Astronautical Congress

6. Oumer, N. & Panin, G. (2012) *3D point tracking and pose estimation of a space object using stereo images*, IAPR International Conference on Pattern Recognition (ICPR)

7. Rank, P. & Mühlbauer, Q. & Naumann, W. & Landzettel, K. (2011). *The DEOS Automation and Robotics Payload*, 11th Symposium on Advanced Space Technologies in Robotics and Automation